

Date: 6/16/17

## EIC Detector R&D Progress Report

**Project ID:** eRD1

**Project Name:** EIC Calorimeter Development

**Period Reported:** from 1/1/17 to 6/30/17

**Project Leaders:** H.Z. Huang and C. Woody

**Contact Person:** H.Z. Huang and C. Woody

### Collaborators

***S.Boose, J.Haggerty, J.Huang, E.Kistenev, E.Mannel, C.Pinkenberg,  
M.Purschke, T. Shimek, S. Stoll and C. Woody***  
(PHENIX Group, BNL Physics Department)

***E. Aschenauer, S. Fazio, A. Kiselev***  
(Spin and EIC Group, BNL Physics Department)

***Y. Fisyak***  
(STAR Group, Physics Department)  
Brookhaven National Laboratory

***F. Yang, L. Zhang and R-Y. Zhu***  
California Institute of Technology

***A. Ali, M. Carmignotto, T. Horn, A. Mkrтчhyan, I. Pegg, R. Trotta  
and A. Vargas***  
The Catholic University of America and  
Thomas Jefferson National Accelerator Facility

***W. Jacobs, G. Visser and S. Wissink***  
Indiana University

***A. Denisov and A. Durum***  
Institute for High Energy Physics, Protvino, Russia

***M. Battaglieri, A. Celentano, R. De Vita, L. Marsicano, P. Musico, M.  
Osipenko, M. Ripani and M. Taiuti***  
Istituto Nazionale di Fisica Nucleare, Sezione de Genova e  
Dipartimento di Fisica dell'Universit`a, 16146 Genova, Italy

***A. Sickles***  
University of Illinois at Urbana Champaign

***C. Aidala, J. Osborn, M. Skoby***  
University of Michigan

***Z.Shi***  
Massachusetts Institute of Technology

***A. Brandin***  
MEPHI, Moscow, Russia

***C. Munoz-Camacho***

**IPN Orsay, France**

***S. Heppelmann***  
**Pennsylvania State University**

***C. Gagliardi***  
**Texas A&M University**

***R. Esha, H.Z. Huang, Md. Nasim, M. Sergeeva, S. Trentalange, O. Tsai, and  
L. Wen***  
**University of California at Los Angeles**

***Y. Zhang, H. Chen, C. Li and Z. Tang***  
**University of Science and Technology of China**

**S.Kuleshov**  
**Detector Laboratory of UTFSM, Valparaiso, Chile**

***H. Mkrtychyan***  
**Yerevan Physics Institute**

## Overview

Full azimuthal and pseudo-rapidity coverage with an EMCAL is essential for EIC science as demonstrated in many simulations by the BNL spin group previously. The eRD1 Collaboration -- EIC Calorimeter Consortium has been working on various detector technologies: the W-Powder/Scintillating Fiber EMCAL at mid-rapidity for compactness and good energy/timing resolutions;  $\text{PbWO}_4$  crystals for the forward electron scattering direction because of superior energy resolution. We report our progress from our ongoing R&D projects: W-Powder/Scintillating Fiber based EMCAL development by the BNL team and the UCLA team; and the  $\text{PbWO}_4$  crystal calorimeter development by the CUA/Orsay team. Research teams led by the UTFSM group and by the INFN-Genova group expressed interest to join the EIC Calorimeter Consortium. They propose new projects on Shashlik EMCAL development as a possible alternative technology at mid-rapidity and on development of triggerless DAQ system, respectively. Their proposals will be submitted separately.

The W-Powder/Scintillating Fiber EMCAL R&D includes efforts from the BNL team and from the UCLA team. This detector technology is suitable for a barrel EMCAL at mid-rapidity. A special prototype aiming at better energy resolution was built and tested by the UCLA team as well. Such a high resolution version of the EMCAL design may be suitable for forward pseudo-rapidity region in the electron-going direction. In the period of Jan-Jun 2017, the BNL team has been focusing on the sPHENIX EMCAL detector prototype and beam testing. The design of the EMCAL module is 2D-projective geometry, which is specifically for sPHENIX in the large pseudo-rapidity region. A beam test run was carried out at FNAL in Jan.-Feb. 2017. Much information has been learned about the module construction techniques and about the readout scheme performance. In the coming period, an improved 2D-projective prototype will be constructed and a new readout scheme with better light collection uniformity will be designed. Another beam test run at FNAL will be scheduled for early 2018. This effort is funded by the sPHENIX project. This sPHENIX specific project continues to learn valuable lessons about construction techniques of Tungsten-Powder/Scintillating Fiber detector modules and to provide independent evaluations of the readout schemes.

The UCLA team focused on the optimization of the light collection scheme using SiPMs for the EMCAL design at mid-rapidity and the evaluation of the SiPM performance in the RHIC collider environment at the STAR IP. By a special arrangement of the fibers and a coupling media with high reflective index between the light guide and the SiPM the UCLA team achieved the desired light collection uniformity and light collection efficiency. To study the SiPM performance under the RHIC radiation environment at STAR IP, a significant number of SiPM readout boards were exposed to the collider environment at the STAR IP. We have identified several issues of SiPM performance degradation relevant for applications in the EIC forward direction. More investigations will follow in the next period of six months.

The CUA/IPN Orsay team working on a high resolution crystal calorimeter for EIC focused its effort on setting up its infrastructure for crystal testing and using it to understand the crystal to crystal variations and systematic effects in crystals from different suppliers (SICCAS and Crytur). This benefitted from the synergy between our EIC R&D effort and the NPS experiment at JLAB and PANDA to provide a

significant number of crystals for testing. In addition, various chemical and materials analyses were performed on some of these crystals. The future plans for this team is to build and test a small array of crystals (5x5 or larger) of the type that would be suitable for EIC, equip this array with photosensors (SiPMs and/or APDs), front end electronics and a readout system, and test this detector in test beam to measure its performance. The goal is to obtain an energy resolution in the range of 1.0-1.5 %/ $\sqrt{E}$  with a constant term  $\sim 0.5\%$  with a time resolution  $< 2$  ns as required for a future EIC detector.

For FY2018, the requested budget numbers are \$49k for the UCLA team, \$148k for the CUA crystal team. The overall budget request from the eRD1 collaboration – EIC Calorimeter Consortium is modest given the proposed R&D scopes involved. The proposed R&D activities cover the full spectrum of various calorimeter technologies necessary for a full kinematic coverage of an EIC detector.

**Overall Cost Matrix (FY18, 100% Funding Scenario):**

<b>Institution</b>	<b>W/SciFi R&amp;D (\$K)</b>	<b>Crystal R&amp;D (\$K)</b>	<b>Sum(\$K)</b>
<b>UCLA</b>	49.0		49.0
<b>BNL</b>		32.0	32.0
<b>CUA</b>		58.0	58.0
<b>Orsay</b>		58.0	58.0
<b>Sum</b>	<b>49.0</b>	<b>148.0</b>	<b>197.0</b>

**Sub Project:** Progress on Tungsten Powder Calorimeter R&D  
by BNL/UIUC/Michigan/MIT Team

**Project Leader:** C. Woody

**Past**

**What was planned for this period?**

Our main goal for this R&D period was to build and test a new large  $\eta$  prototype of the sPHENIX EMCAL and test it in the test beam at Fermilab. Large  $\eta$  prototypes of the sPHENIX EMCAL, Inner HCal and Outer HCal, along with a mockup of the superconducting solenoid magnet, representing a rapidity region around  $\eta \sim 0.9$  in the final detector, were tested in the beam during January-February of 2017. The main part of this test that is related to EIC calorimeter R&D is the W/SciFi EMCAL that is also planned to be used as a Day 1 detector at eRHIC.

The EMCAL prototype consisted of a 4x4 array of absorber blocks (8x8 readout towers) produced at the University of Illinois at Urbana Champaign. The blocks are designed to be projective in two dimensions ( $\eta$  and  $\phi$ ), although in their final configuration in sPHENIX, they will be arranged so that they are not perfectly projective back to the vertex. Figure 1 (left) shows the absorber blocks after gluing on the light guides to the readout end. Half of the calorimeter was equipped with 1" long trapezoidal light guides that were produced by an inexpensive injection molding process, while the other half were equipped with high quality 2" long machined and polished light guides. This was done in order to test the effect of the light guides and their light collection uniformity on the measured energy resolution. The photo on the right in Figure 1 shows the blocks after being installed inside the prototype enclosure with the readout electronics attached. Figure 2 shows the test setup with EMCAL, Inner HCal and Outer HCal prototypes at the Fermilab Test Beam Facility.

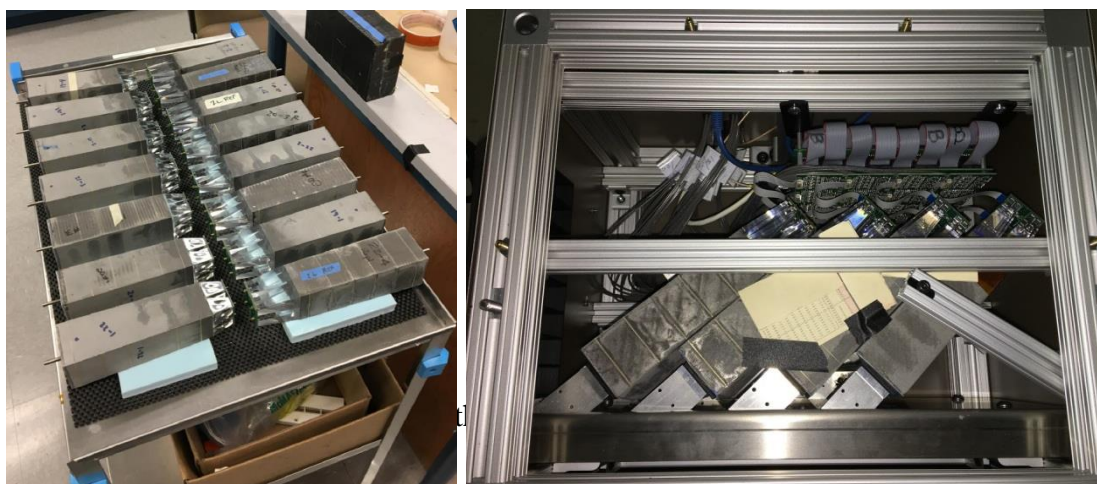


**Figure 1.** 2D projective absorber blocks for the large  $\eta$  configuration of the sPHENIX W/SciFi EMCAL. Left: Absorber blocks after gluing on light guides to readout end. Right: After installation into prototype enclosure with readout electronics attached.

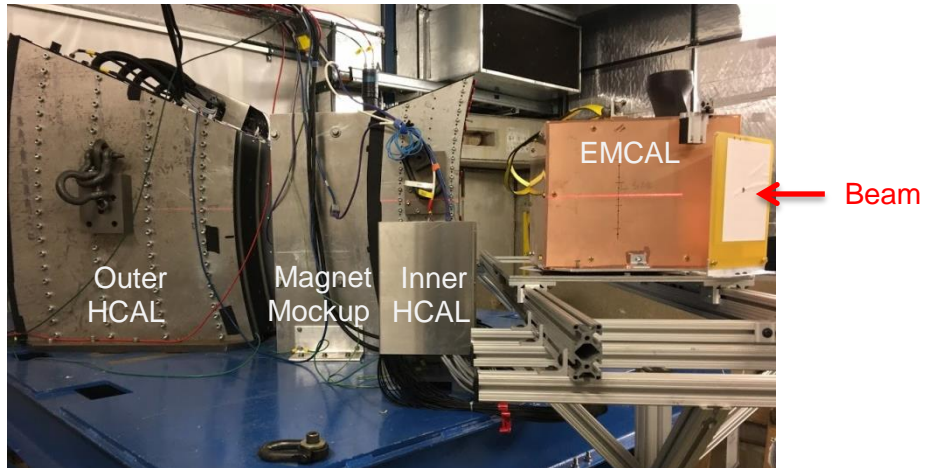


**Figure 2.** Test setup with the prototype EMCAL, Inner HCAL, magnet mockup and Outer HCAL at the test beam at Fermilab.

### What was achieved?

The beam test at Fermilab was successfully completed in Jan-Feb 2017 as planned. The EMCAL prototype was tested in a standalone mode in order to measure its performance over the energy range from 1-16 GeV, and also in combination with the sPHENIX HCAL prototype. Figure 3 shows some preliminary results on the energy resolution from the standalone test. The curve on the left shows the energy resolution using the sum of 5x5 towers centered over a region of the detector that includes light guide boundaries but not block boundaries. The curve on the right shows the resolution including both light guide and block boundaries. The curves labelled “recalib” have had a position dependent correction applied using the known incident beam position using a scintillation hodoscope in front of the calorimeter. With this correction, the energy resolution comes down to  $13.0\%/\sqrt{E} \oplus 1.6\%$  after unfolding the beam momentum spread of 2% in the case of only the light guide boundaries, and  $15.6\%/\sqrt{E} \oplus 4.3\%$  in the case of both light guide and block boundaries. The green curve shows a Monte Carlo simulation with a flat light collection response.

The energy resolution, especially the constant term, worsens when the block boundaries are included. In order to study this, we measured the energy response as a function of position over the entire central region of the calorimeter using 8 GeV electrons. Figure 4 shows the result of this study. The plot on the left shows the energy response with the beam incident at  $0^\circ$  (i.e., normal to the front face) and the plot on the right shows the response with the beam incident at an angle of  $10^\circ$  in the horizontal plane. The black square indicates one of the central blocks, where the light guide boundaries are indicated by the black dashed lines inside.

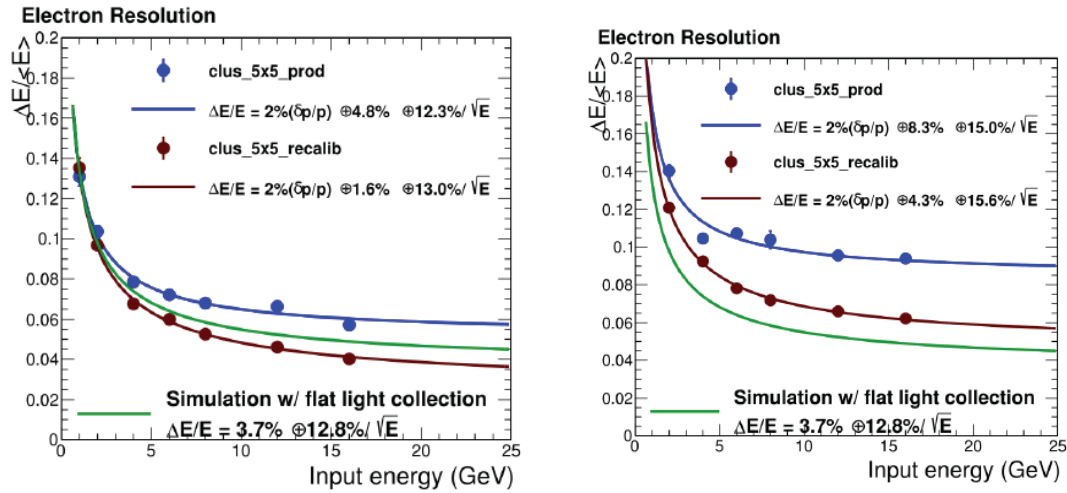


**Figure 3.** Preliminary results on the energy resolution for electrons measured with the large  $\eta$  EMCAL prototype. Left: Covering a region of the detector that includes light guide boundaries but not block boundaries. Right: Covering a region that includes both light guide and block boundaries. “Recalib” is with a position dependent correction applied. The green curve is a Monte Carlo simulation with a flat light collection response.

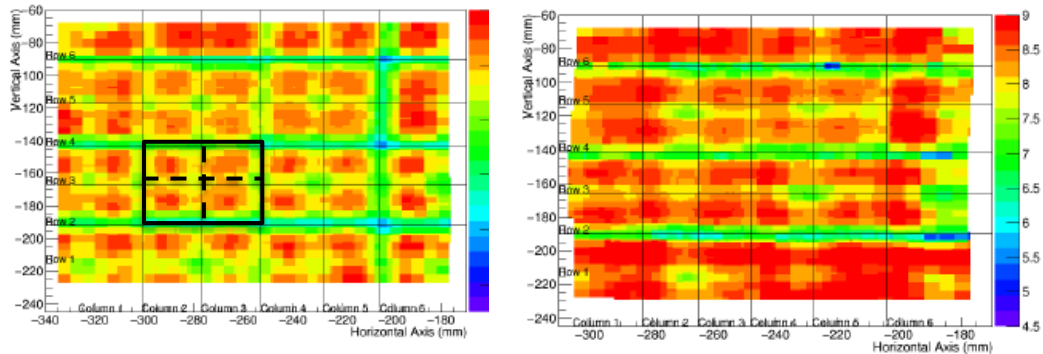


**Figure 4.** Energy response for 8 GeV electrons as a function of position for the central region of the calorimeter. Left: Beam incident at 0°. Right: Beam incident at 10° in the horizontal plane. Black square indicates one of the central blocks with the light guide boundaries inside. The upper half of the plots are the blocks that had the 2” light guides and the bottom half had the 1” light guides.

This study revealed an intrinsic feature of this type of calorimeter, which is that it has a strong position dependence that has a direct effect on the energy resolution. We believe that this is due to the non-uniformities in the light collection using the short trapezoidal light guides with 4 SiPMs, and from the dead regions at the boundaries between the blocks. We do not believe that non-uniformities with the absorber block have any significant effect on the energy resolution or uniformity of response. The effect of the boundaries in this prototype was worse than we expect in the final calorimeter and we have plans on how to improve this in the next prototype as described below. However, as indicated in the right hand plot in Fig. 4, when the detector was rotated in the horizontal plane such that the beam entered at an angle of 10°, the uniformity improved dramatically in that direction.

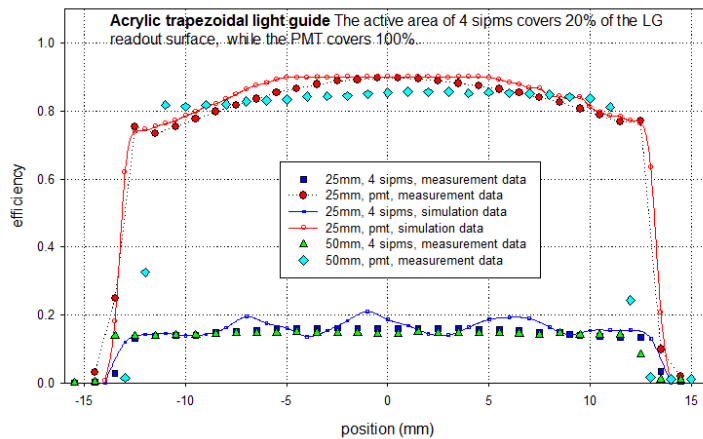


**Figure 5.** Comparison between simulation and lab measurements of the light collection uniformity across the central region of 1” and 2” trapezoidal light guides using a PMT with full coverage of the readout end and with 4 SiPMs.

We saw very little difference in the non-uniformity between the 1” and 2” light guides. The top half of both plots in Fig. 4 are the blocks that had the 2” light guides and the bottom half had the 1” light guides. We also studied the light collection uniformity of the trapezoidal light guides using a ray tracing program (TracePro) and compared the results to lab measurements. Figure 4 shows some results from this study and gives the same conclusion. We also compared other shapes of light guides, including various Winston cone geometries, and found that the best uniformity for a short 1”-2” light guide read out with 4 SiPMs was still a simple trapezoid.

We are planning to try and improve the light collection uniformity by arranging for the fibers to taper slightly inward at the readout end of the block, similar to what was tried by the UCLA group. This requires an additional step in the manufacturing process of adding a plastic frame at the front of the block to slightly bend the fibers at one end inside the mold, but this seems to be possible to do without too much difficulty. Figure 6 shows a sample block made incorporating this procedure into the production process. Reducing the fiber area inside the block also has the added benefit that the readout area can be arranged to be the same for all blocks of different shapes, allowing them all to use the same type of light guide.

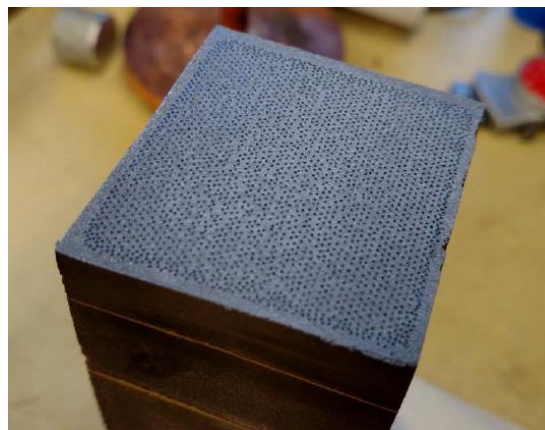


**Figure 6.** 2D tapered block with fibers bent slightly inward towards the center of the readout end of the block to improve light collection uniformity.

## **What was not achieved, why not, and what will be done to correct?**

Because the beam test was scheduled in mid January 2017 and we could not start to produce the absorber blocks until the Fall of 2016, we did not have time to fully develop the procedure for making the 2D projective blocks before the beam test. Therefore, the blocks that were tested were some of the first 2D projective blocks ever produced had many imperfections and problems, including large dead areas around the edges of the blocks, which worsened the effect of the block boundaries. In addition, the procedure for infusing the blocks with epoxy was found to be not ideal and led to possible voids inside the blocks along with various other problems.

We now plan to produce a second 2D projective large  $\eta$  prototype with new absorber blocks made with an improved technique, including with the tapered fibers at the readout end, and test this prototype at Fermilab in early 2018. We also plan to have new light guides produced by a company that specializes in injection molded optical quality parts. We have seen samples of other parts made by this company and they look to be of excellent quality. If these light guides turn out to be satisfactory, this will allow us to produce one, high quality mold for all the light guides in our final calorimeter and obtain them at a very reasonable cost. The new prototype will incorporate all the changes and improvements based on what we learned from the previous prototype and will hopefully have better energy resolution and uniformity of response.

## **Future**

### **What is planned for the next funding cycle and beyond? How, if at all, is this planning different from the original plan?**

Our main activity during the next six months will be to construct the new large  $\eta$  prototype calorimeter and prepare it for our beam test next year at Fermilab. We will also begin construction of a full scale preproduction prototype consisting of one complete sector of the sPHENIX EMCAL. The construction of this prototype will continue into next year, but we do not plan to test this prototype in the test beam. These activities are all proceeding according to the overall construction schedule for sPHENIX.

### **What are critical issues?**

The most critical issue for sPHENIX during the next six months will be to build the new large  $\eta$  prototype and test it in the beam at Fermilab. This will tell us the overall performance we expect from the final detector. The second critical issue will be to construct the preproduction prototype which will give us the knowledge and experience required to build the full 64 sectors for the final sPHENIX detector.

## **Manpower**

*Include a list of the existing manpower and what approximate fraction each has spent on the project. If students and/or postdocs were funded through the R&D, please state where they were located, what fraction of their time they spend on EIC R&D, and who*

*supervised their work.*

The group from UIUC continues to play a major role in the development of the EMCAL for sPHENIX, and the group from the University of Michigan has now also joined this effort. A group from Debrecen University in Hungary is also playing a significant role in developing the SiPM readout for both the sPHENIX EMCAL and HCAL, and has also made a significant contribution to the study of radiation damage in SiPMs. T.Shimek and Z. Zhi were graduate students that made important contributions to this effort during this last period.

## **External Funding**

*Describe what external funding was obtained, if any. The report must clarify what has been accomplished with the EIC R&D funds and what came as a contribution from potential collaborators.*

The R&D on the sPHENIX calorimeters is being completely supported by sPHENIX funds and our work on radiation damage in SiPMs has been partly supported by a BNL LDRD. We do not request any support from EIC R&D funds for the next Fiscal Year.

## **Publications**

*Please provide a list of publications coming out of the R&D effort.*

A contribution was submitted to the Proceedings of the 2016 CALOR Conference on the first beam test of the sPHENIX EMCAL prototype. These proceedings are now in process. A second, more complete paper on the test beam results of the entire sPHENIX calorimeter system (EMCAL+HCAL) was submitted to the IEEE Transactions on Nuclear Science in March 2017 and is currently under review. A contribution on a Monte Carlo study of various light guide geometries was submitted to the 2017 IEEE Nuclear Science Symposium and Medical Imaging Conference, and a paper on radiation damage studies in SiPMs is currently in preparation and will be submitted to the IEEE TNS later this year.

**Sub Project: Progress on Tungsten Powder Calorimeter R&D**  
by the UCLA/BNL/IU/PSU/TAMU team  
**Project Leader: H.Z. Huang and O. Tsai**

**What was planned for this period?**

- Optimization of light collection scheme for FEMC.
- Study performance of FEMC readout in a collider environment close to that expected at EIC.

**What was achieved?**

We have achieved the goals planned for the past 6 months: optimization of the light collection scheme and evaluations of SiPM readout at RHIC radiation environment. Optimization of the light collection scheme for FEMC has completed. The FEMC prototype was equipped with triple readout and placed in the STAR IP for the RHIC 500 GeV run at a distance of 125 cm from the beam line. Extra calorimeter blocks were placed very close to the beam line, at a distance of 35 cm ( $\eta \sim 3.75$ ). Calibrated SiPM boards were placed in these locations and were removed at various times during the run. As a result, they have different radiation dose exposures. A number of shielded and unshielded SiPMs were placed near the beam line, along with APDs. On the opposite side of the STAR IP, both STAR pre-shower and post-shower detectors were read out with SiPMs. CERN radiation monitors were placed in these locations to track dose rates and neutron fluence. The information from these STAR subsystems was recorded and is available for further analysis. As of early June, we are still taking data and expect Run 17 to end in late June. The results shown in this report were obtained from only a small fraction of the SiPM boards placed in the STAR IP and are preliminary.

Optimization of the light collection scheme addresses two questions: uniformity of response and efficiency of light collection. As was shown in our previous reports, the first question is tied to a constant term in the expression for energy resolution. In particular, for high-resolution prototypes, we achieved a constant term at the sub-1% level for a non-projective configuration of the BEMC with a traditional scheme of light collection. A slightly larger constant term was obtained with a non-projective FEMC with a compensation filter between the light guides and scintillation fibers in the compact readout scheme. However, this was achieved by sacrificing efficiency. The efficiency of the light collection is important for keeping both the stochastic term at a desired level and the S/N ratio at acceptable level when the performance of the silicon sensors degrade under irradiation. Therefore, we abandoned schemes with compensation filters and developed a method of controlling irregularities in the arrangement of fibers to achieve the desired uniformity without sacrificing efficiency. Additionally, we found that a coupling media with higher refraction index between SiPMs and light guides can significantly change the uniformity of light collection. A series of scans to measure the uniformity of response for different light collection schemes is shown in Fig. 1. The light source used for these scans had an intensity profile close to the transverse intensity profile of an electromagnetic shower. The new light collection scheme of light is about 4.5 times more uniform compare to the initial scheme. The uniformity of response in the

improved scheme is 1.6% (r.m.s.), which is close to that achieved with the high-resolution prototype in the FNAL test Run in 2016.

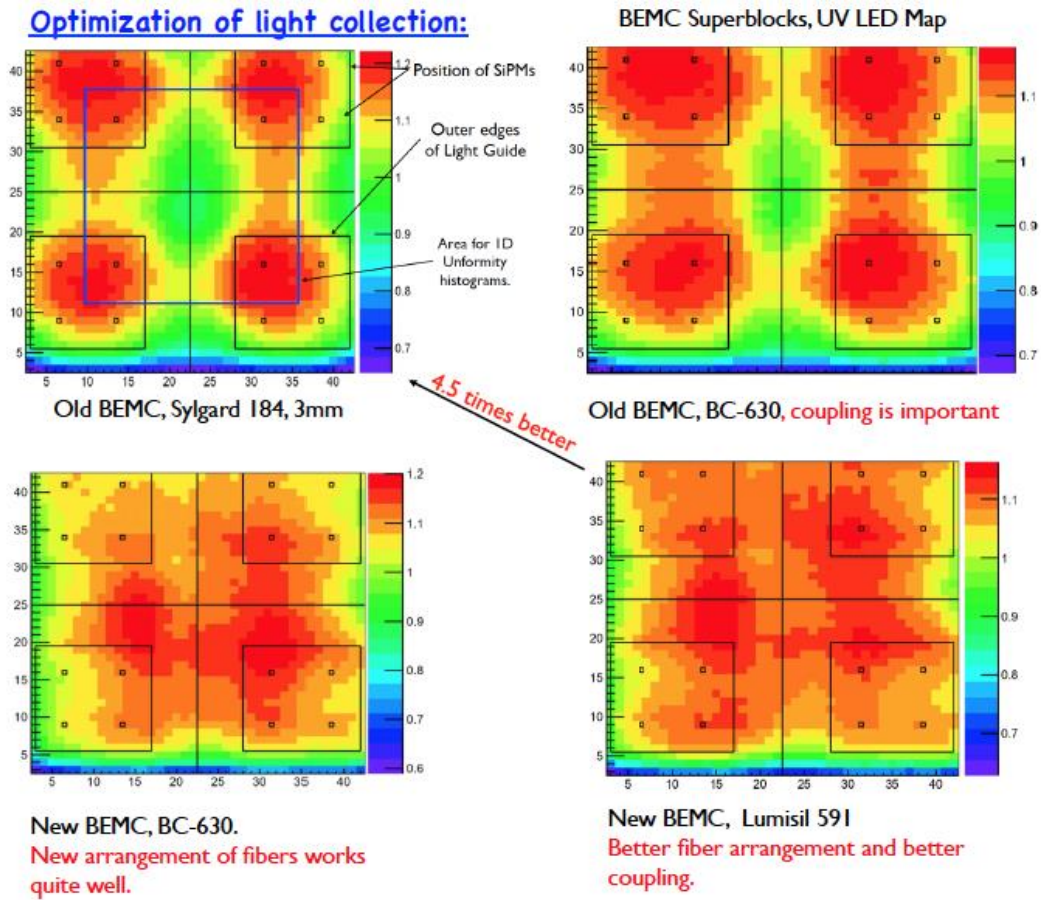


Figure 1. Uniformity of response of BEMC with different arrangement of fibers and different coupling between SIPMs and light guides.

Additional measurements were performed with longer light guides. We found that the non-uniformity in this case increased a bit (Fig. 2), compare to the nominal one-inch long light guide for which we optimized the bending of fibers at the edges and in the middle of the tower. It is possible that the same uniformity and efficiency can be achieved as well by optimizing the bend angles for a longer light guide. However, space in EIC detector is quite limited.

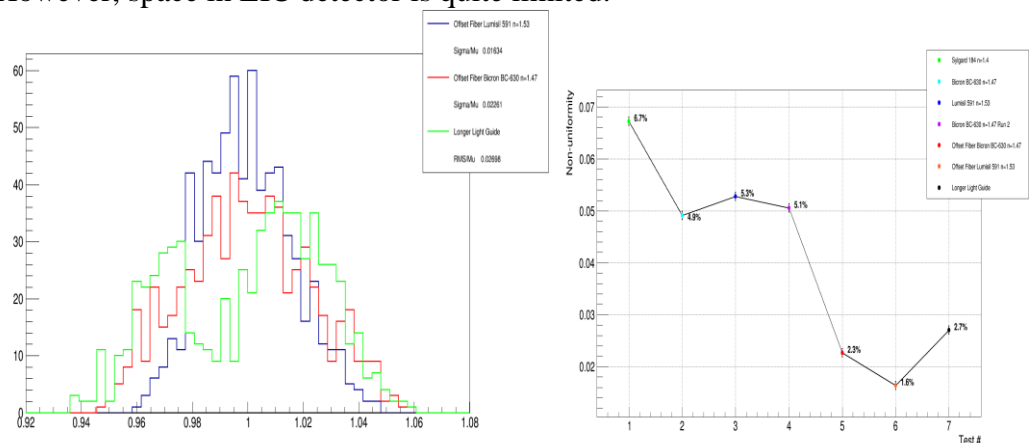


Figure 2. Uniformity of response for different light guides (left). Summary plot (right).

The development of a light collection scheme for a non-projective central EMCAL is in good shape and future improvements can be made at later stages. For forward calorimeters, the situation is becoming more complicated, primarily due to the significant degradation of performance of SiPMs observed in Run 17 from radiation damage.

As we reported earlier, neutron fluxes in the outgoing hadron direction at EIC are similar to those present at the STAR IP under RHIC environment (preliminary results by A. Kiselev estimated  $10^{10}$  n/cm<sup>2</sup> per year at the start of the EIC program and go up to  $10^{11}$  n/cm<sup>2</sup> at the highest EIC luminosity). This result of neutron fluxes was the main motivation to investigate performances of SiPMs and APDs in the STAR IP during RHIC runs. In our previous reports, we estimated the degradation of performance of W/ScFi EM calorimeters read-out with SiPMs, based on our experience with the SiPMs read-out for the STAR Forward Pre-shower Detector during RHIC Run 15 (pp 200 GeV). The degradation due to increases in SiPMs noise was acceptable. This is probably still true for the central EMCAL at EIC where the neutron fluxes were estimated to be at the level of  $10^9$  n/cm<sup>2</sup>. The degradation of SiPMs performance observed during pp 500 GeV Run17 may force us to reconsider the configuration of the forward calorimeter system for EIC. Unlike the radiation damage in Run 15 (increase in dark noise), we observed further degradation in detector response (i.e., the product of PDE and Gain). Additionally, after-pulses may affect performance of the most central part of the detector where the hit rate will be as high as that observed during Run 17.

In this report we show preliminary results from the sensors which have already been removed from the IP during Run 17. This is a small fraction of all sensors placed in the STAR IP at the beginning of the run. The majority of sensors will be removed at the end of Run 17 (June 30th). Accumulated dose and annealing factors for sensors removed to date are listed in Table 1. Equivalent Noise is calculated assuming a light yield of 500 p.e./GeV. S/N degradation is calculated with respect to un-exposed SiPMs. All numbered SiPM boards were located 125 cm from the beam line, which represents approximately the low eta boundary for forward calorimeters at EIC. Shielded and un-shielded sensors were placed for a one-month exposure at 35 cm from the beam line, which is close to high eta end of forward calorimeters.

SiPM Board #	Date Removed from IP	Annealing Factor $10^{-17}$ (A/cm)	Exposure in $10^{10}$ (n/cm <sup>2</sup> )	Response degradation (HPK,Bias) May 25, 2017	Correction based on initial calibrations Nov7, 2016	Response Degradation Corrected	Eq.Noise (RMS) (MeV)	S/N Degradatio
5	March 16	3.7	2.7	0.99	1.03	0.96	17	1.56
7	March 22	3.75	4.5	1.01	1.02	0.99	20	1.79
13	March 30	3.77	5.8	1.03	1.04	0.99	22.1	1.98
8	April 5	3.8	6.8	0.97	1.01	0.96	23.4	2.15
3	April 20	3.9	8.2	0.99	1.01	0.98	26.8	2.42
4	May 3	4	9.5	0.95	1.02	0.93	28.8	2.73
Unshd.	May 17	4.8	14.8					
Shield.	May 17	4.8	10.6					

**Table 1. Sample of sensors tested up to May 25<sup>th</sup>.**

SiPMs are self-analyzing devices, i.e. from leakage current one can calculate neutron fluence, as we verified in Run 15. There is some uncertainty on accounting for the volume of silicon, particularly the way one treats the areas under the quenching resistors, given by the “fill factor,” as listed in the HPK specifications. The fluences listed in Table 1 assume that the volume scales with the fill factor. We will have better estimates after the relation between the CERN radiation monitors and FPS and FPOST SiPMs are determined.

All characteristics of SiPMs depends on overvoltage. Overvoltage in graphs below are relative to the nominal HPK breakdown voltage.

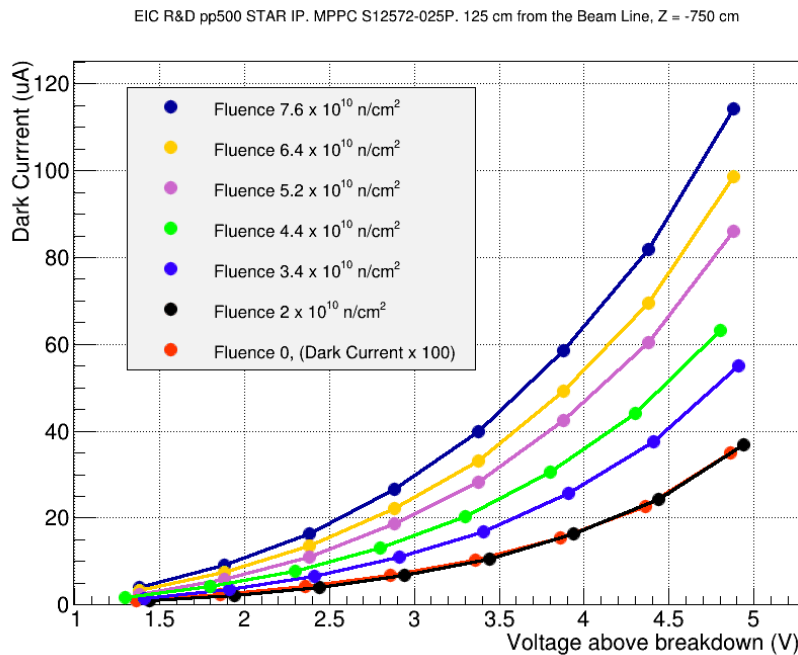


Figure 3. Leakage current per SiPM vs nominal overvoltage for different neutron exposures.

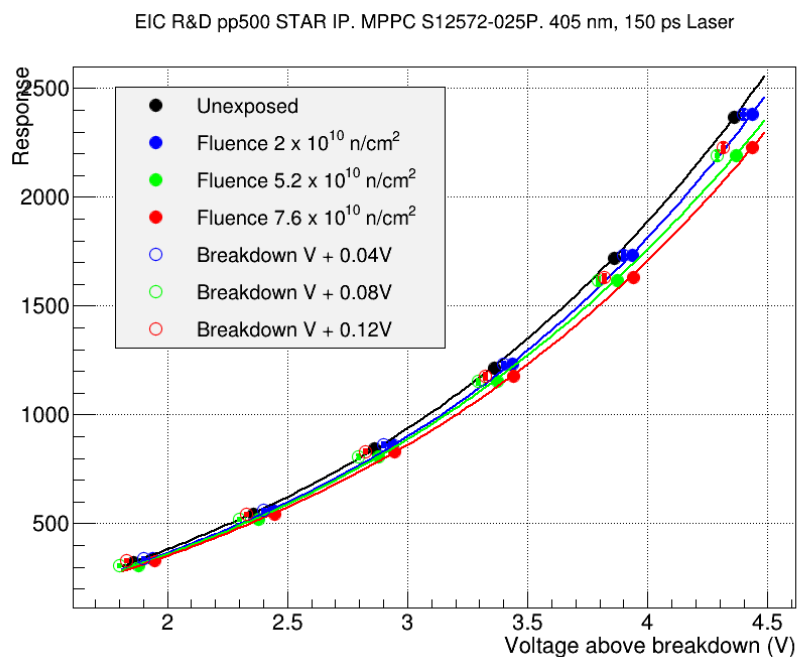
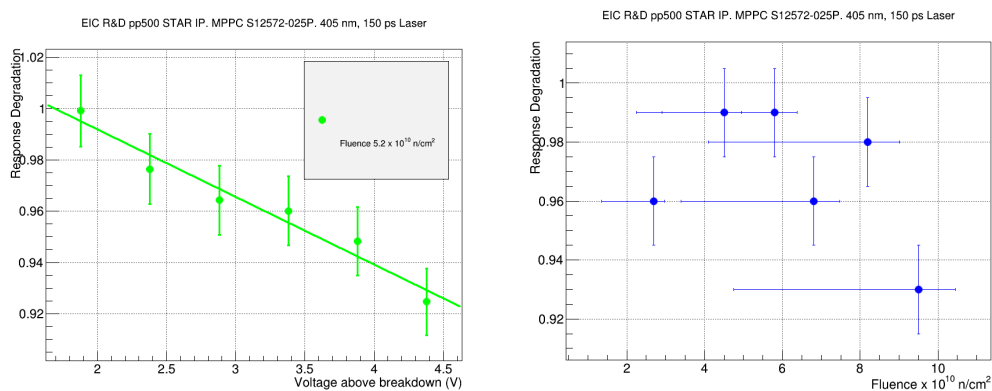


Figure 4. Response to fast light pulse vs overvoltage for different neutron exposures.

Measurements of leakage currents are used to calculate exposure. Note that for unexposed sensors, the leakage currents in Fig. 3 were multiplied by a factor of 100. There are indications that nominal breakdown voltage may change with exposure as well (CMS reported a shift of 175 mV for SiPMs exposed to  $10^{12}$  n/cm<sup>2</sup>, then annealed at 60 degrees C for 1000 hours).

Degradation in response to fast light pulses is clearly observed for SiPMs exposed during Run 17. Qualitatively, the assumption that breakdown voltage changes with exposure may explain the shift in response for region of over-voltage smaller than 3.5 V, as shown with open markers in Fig. 4. At higher over-voltage settings, a simple shift cannot explain the data, as shown in Fig. 5 (left panel). Degradation in response strongly depends on over-voltage. A complete explanation may depend on the roles played by pixel recovery time and duration of the light pulses. We plan to run similar tests with light sources mimicking light pulses from the detector, because degradation as seen with 150 ps laser pulses may be different from that for real signals. It is necessary to investigate this since, at least in case of HCAL, light pulses from the detector will have different shapes depending on the e.m. fraction in the signal.



**Figure 5. Degradation of response vs over-voltage (left). Degradation of response at 3.5 over-voltage for different exposures (right).**

With the limited number of samples tested so far, we clearly see degradation in the response with increases in exposure, as shown in Fig. 5 (right panel). Unfortunately, preliminary results pose more questions than answers. **The most important one: are different sensors degrading the same way with exposure?** With the current readout scheme of four SiPM per tower, differential degradation of sensors will lead to an increase in constant term for the energy resolution, i.e. the same question of non-uniformities of response when we discussed the light collection scheme. There is a curious observation at this stage: six sensors which were shielded with two inch thick HDPE showed almost the same increase in leakage currents [54,55,57,55,57,57 uA], while six unshielded SiPMs located at the same spot have a much wider spread in their leakage currents [68, 82, 75, 80, 90, 85 uA]. We have not had time to measure response to laser pulses for these sensors yet.

The other obvious complication with degradation in response of SiPMs is the design of a monitoring system. Sensors placed 35 cm away from the beam pipe received more damage in one month than sensors locate 125 cm away in two and a half months. The rudimentary monitoring scheme we originally envisioned will not be

suitable to track these details. A more advanced scheme will put additional constraints on the already-limited space in the EIC detector.

Increased noise with the radiation exposure complicates a lot of things, both for EMCAL and HCal. For example, our previous readout design for HCal is probably unusable if conditions at EIC are close to those we have at present in the STAR IP. With eight SiPMs per tower, we measured a light yield of 140 p.e./GeV at the FNAL test run in 2014. Scaling board #4 in Table 1, which has four SiPMs, the equivalent noise for HCal is already 145 MeV. Potentially we would already lose the ability to detect MIPs, which is the primary method to calibrate HCal towers. Reducing the gate width obviously decreases the noise, as shown in Fig. 6 (left). In this case, the SiPM signal was fed directly to the ADC. Based on measurements for a single board, it is not obvious that there is an optimal bias setting. In fact, there is an indication that with smaller over-voltage, one can get better S/N as shown in Fig. 6 (right) panel. Note that the after-pulses probability is proportional to  $\Delta V^2$ .

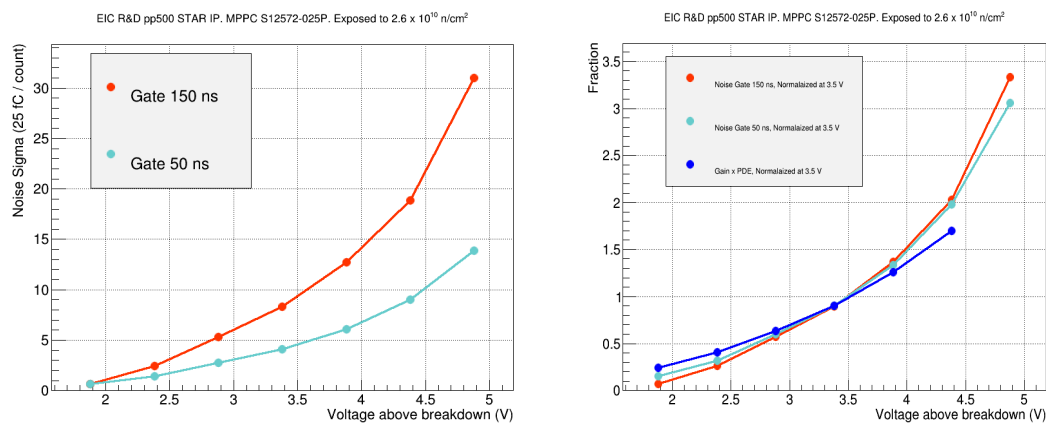


**Figure 6.** Noise with different gate width (left). Changes in noise and response which are normalised at 3.5 V over-voltage (right).

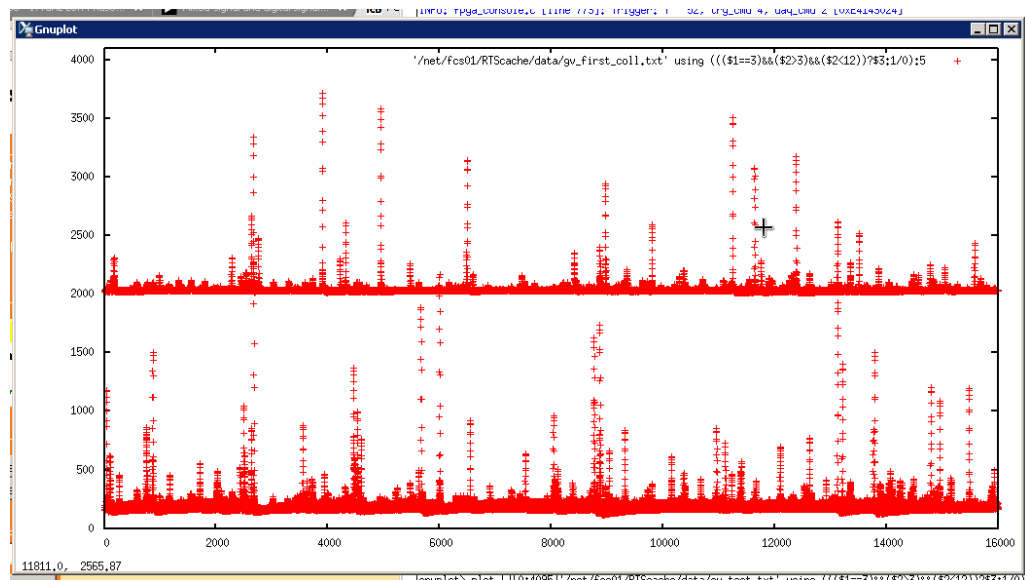


**Figure 7.** Hit rate in four 5x5 cm<sup>2</sup> tower, over a time window of 213 uS. STAR IP Run 17.

There is an additional concern when using SiPMs in the forward direction. SiPMs, unlike other silicon sensors, have a problem with after-pulses. Combined with

formation of deeper level traps it can potentially create additional issues for calorimeters in the forward direction subjected to high particle rate and machine backgrounds.

Figure 7 gives an example of the scale of these difficulties. We measure the detector response for towers located 35 cm from the beam line in Run 17 with an STAR 80 MHz WFD. The average frequency of hits is  $\sim 100$  kHz for a  $5 \times 5$  cm<sup>2</sup> tower. Many pile-up and after-pulses are present and their effects must be quantified.

Finally, we conclude on the discussion of the SiPM performance on a positive note. We did not observe excess signals due to primary ionizations in silicon for the FEMC equipped with triple readout. In Run 17, we compared the responses of 64 SiPMs collecting scintillation light to 64 blind SiPMs located right next to them, and both in correlation with a PMT which was triggered on the same scintillation light as the SiPMs. The threshold for individual signal was set at three sigma above pedestal.

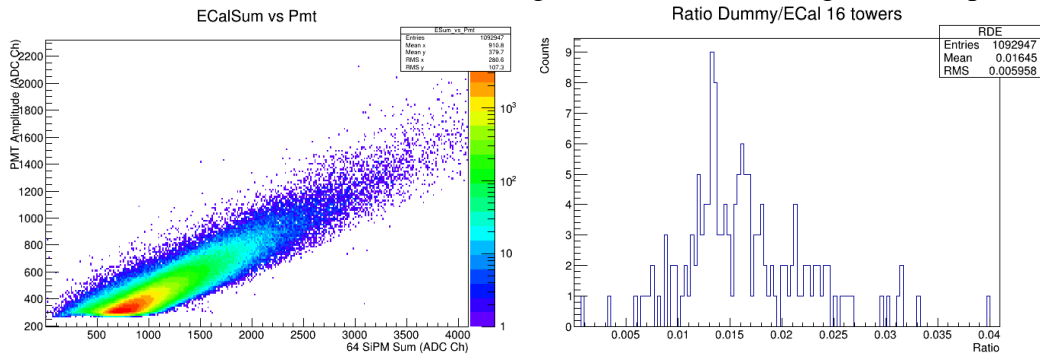


Figure 8. Correlation between PMT and SiPMs signals (left). Ratio of Dummy to normal SiPMs (right).

As shown in Fig. 8 for only a small fraction of events ( $\sim 10^{-4}$ ), the ratio of the sum of the signals from 64 dummy SiPMs to the sum of the signals from 64 SiPMs collecting scintillation light is 1.6%. Thus, combined measurements during Run 16 and Run 17 confirmed that SiPMs are insensitive to nuclear counting effects, unlike APDs.

### Discussion.

Although results in this report are still preliminary because only a small fraction of the exposed sensors have been characterized so far, we learned that current SiPMs may not be an optimal choice as a photo-detector for forward calorimeters at EIC. This is true for HCAL in outgoing hadron direction, and is probably true for EMCAL in the hadron direction as well. There is a concern for the outgoing electron direction as well where much better resolution from calorimeters is required. Three effects including the increase of noises, the degradation of responses and after-pulses may significantly affect the SiPM performance if used for forward calorimeters at EIC.

The usual way to improve S/N is to increase light yield and to decrease the volume of silicon sensors used to collect light. Unfortunately, in SiPM case this approach is not valid because in order to satisfy required dynamic range one inevitably would have to increase the number of SiPMs to collect light from the detector. The biggest concern at this moment is potential differential degradation of SiPMs under exposures.

In case of HCAL readout we conclude that APDs would be a better choice, despite the fact that they are sensitive to NCE as we reported after tests in STAR IP in 2016. With optimized sensor configuration and modified light collection scheme for HCAL we may be able to significantly improve S/N as compared to our previous scheme of readout. This however will require to double the number of readout channels in HCAL due to separate readout of two APDs collecting light from the same tower.

## Future Plan

In next six months, we plan to characterize all exposed SiPMs in the lab. In total, we will have about 160 SiPMs exposed in Run 17 at 125 cm and 35 cm away from the beam line and a few S8664-55 APDs. This sample is sufficient to answer the questions we discussed previously, which include:

- Main concern: Is degradation in responses the same for sensors located at the same position?
- Do we see change in  $V_b$  and is the change same for different sensors?
- Does degradation in responses depend on shapes of light pulses?
- Noise as a function of  $\Delta V$  and gate width.
- Effect of increased after pulses, trap lifetime and high particle rate.
- Excess noise factor, by direct comparison of responses of HCAL and EMCAL to cosmic muons (exposed/unexposed sensors, both SiPMs and APDs).
- In longer term, consider cooling and may be shielding.
- Define requirements for a comprehensive monitoring system.

For the next RHIC Run we propose to prepare two HCAL towers with dual readout (PMT/APDs). The goal is to verify that with two APDs per tower we can mitigate effects associated with NCE. We already started to modify the HCAL light collection scheme in order to increase the light yield significantly.

Calorimeters by themselves are a major source of neutrons. The number of generated neutrons strongly depends on chemical composition, i.e. whole idea of compensation is based on generating large number of neutrons in high Z materials, like lead and uranium. We advocated for a compensated system for EIC, however if silicon sensors is the only option to readout the forward calorimeters (magnetic field and lack of space) we should reconsider in favor of non-compensated designs, i.e. replace lead with iron to reduce neutron fluxes. Once we finish characterization of sensors, we would have a better idea how to proceed. Several things would have to be pursued:

- MC to optimize composition.
- We need reliable MC to calculate neutron fluxes, tied to IP design.
- We also need to know rates and possible effects of machine background in the forward region.
- With a non-compensated calorimeter system, energy reconstruction becomes more complicated, sophisticated approach such as machine learning can be used.
- Timing structure of signal, understand requirements on readout electronics.
- Requirements from jet measurement.

- As part of the design for a comprehensive EIC detector system, it should be a global discussion regarding envelopes for each subsystem at EIC. The space is very limited; as we mentioned in this report adding cooling/shielding and advanced monitoring systems all will require space.

### **Budget.**

Below we list our budget request for FY18 in 3 budget scenarios. The first is assuming full funding is available, and the other two scenarios assume a 20% cut and 40% cut respectively.

Budget scenario	100%	20% cut	40% cut
Hamamatsu Sensors	\$15k	\$7k	\$0
UCLA Electronics Shop (26% overhead included)	\$6.3k	\$4.6k	\$1.7k
UCLA support for students (26% overhead included)	\$15.1k	\$15.1k	\$15.1k
Travel (26% overhead included)	\$12.6k	\$12.6k	\$12.6k
Total Direct	\$42.0k	\$30.9k	\$21.8
Total	\$49.0k	\$39.4k	\$29.4k

**Sub Project:** Crystal Calorimeter Development for EIC based on  
PbWO<sub>4</sub>

**Project Leader:** Tanja Horn

*High resolution calorimetry is critical at the EIC in the two endcaps for particle identification and reconstruction.* In the electron endcap, particle identification is important for discriminating single photons from, e.g., DVCS and two photons from  $\pi^0$  decay, and e/p. Resolution is essential for particle reconstruction, which is driven by the need to accurately reconstruct the four-momentum of the scattered electrons at small angles. There, the angular information is provided by the tracker, but the momentum (or energy) can come from either the tracker or the electromagnetic calorimeter. At rapidities  $< -3$  the energy measurement comes mainly from the calorimeter. As described in our January 2017 report, resolution helps to extend the useful y-range and “purity” in x/Q<sup>2</sup> bins. To make a clear positive impact on the scattered electron kinematics determination the requirements on the inner calorimeter are:

1. Good **resolution in angle** to at least 1 degree to distinguish between clusters,
2. **Energy resolution** (1.0% – 1.5%)/ $\sqrt{E}$  + 0.5% to measure cluster energy,
3. **Time resolution** to  $< 2$  ns
4. Ability to withstand radiation down to at least 1 degree with respect to the beam line.

A solution based on PbWO<sub>4</sub> is optimal due to its small Moliere radius ( $R_M=2.0$  cm), high density (8.3 g/cm<sup>3</sup>), fast response, and radiation resistance.

The critical aspect for **crystal quality, and thus resolution performance** of the EIC inner endcap calorimeter, is the combination of high and uniform light output and radiation hardness, which depend on the manufacturing process. Our previous studies have shown that there is significant crystal-to-crystal variation for crystals manufactured by SICCAS. *Evaluation of the variation from crystal to crystal and possibly determining the origin of it is thus one of the main goals of this R&D project.* This information will be important for what is acceptable for the EIC inner endcap calorimeter. Our previous studies also showed that the constant term, which includes several systematic effects like nonlinearities in light collection, which are in part properties of the crystal itself, has a large impact on the response parametrization. *Another main goal of this R&D project over the next year is thus to explore ways to reduce the constant term.* The construction of a prototype and availability of a sufficient number of quality crystals is critical. The prototype will allow for studies of the crystals in test beam and measure the actual energy and position resolution, to investigate possible reductions of the constant term, and to test different readout systems.

Assuming that our FY18 crystal quality tests are completed successfully and one or two vendors capable of producing such crystals have been identified, the crystal calorimeter R&D will focus in subsequent years on the optimization of

geometry, cooling and choices of readout system of the endcap inner crystal calorimeter.

## **Past**

### **What was planned for this period?**

- We had planned to finalize setting up the infrastructure for crystal testing, e.g., at IPN-Orsay and CUA, and to understand systematic effects in the characterization of SICCAS produced crystals since 2014.
- We had planned to procure a reasonable batch of full-sized crystals from Crytur and evaluate their crystal-to-crystal variation including the impact of impurities on crystal performance.
- We had planned to construct a prototype to study crystals from either SICCAS or Crytur in test beam and measure the actual energy and position resolution that we could achieve with them.
- We had planned to test different readout systems (SiPM, APD, PMT) for the EIC crystal inner calorimeter using the prototype.

### **What was achieved?**

With commitment of internal university and laboratory funds and through synergy with the NPS project at JLab we managed to partially carry out crystal characterization for crystal specifications and impact on EIC detector performance at CUA and IPN-Orsay, as well as work towards constructing a prototype to establish limiting energy and position resolutions and to test different readout systems. Our activities were:

- Work towards finalizing the infrastructure for crystal testing at CUA and IPN-Orsay, and initial studies towards understanding crystal-to-crystal variations and systematic effects in SICCAS and Crytur crystals. We summarize methods and availability of instrumentation in the appendix.
- Tested two methods of crystal chemical analysis and obtained initial results on contribution of impurities and defects, as well as stoichiometry. Work towards developing non-destructive sampling methods for chemical analysis
- Work towards construction of a prototype to test different readout systems. Preliminary measurement of light output of one PWO crystals with photodiodes at CUA. Tested SiPM readout with beam at Fermilab.

## **What was not achieved, why not, and what will be done to correct?**

- We made good progress on characterization of crystals produced by SICCAS (since 2014) and understanding systematic uncertainties in our methods. In anticipation of the next phase of crystal testing and with support from the VSL and JLab (NPS project), we procured 460 additional crystals from SICCAS in 2017 and components for our crystal testing facility at CUA. Similarly, IPNO procured components and setup space for crystal testing at IPN-Orsay. We are planning to work within the constraints of the approved budget for FY17 to complete our studies of systematic uncertainties between setups and impact of chemical composition on crystal performance.
- We have obtained a full-size, later growth cycle crystal from Crytur and made initial measurements to determine if such crystals would be suitable for EIC. The results are encouraging, but an evaluation of the crystal-to-crystal variation for this type of crystal was not possible with one sample. In collaboration with the NPS and PANDA experiments, we are planning to further explore the potential of late growth cycle crystals.
- We made some progress towards the construction of a single-crystal prototype to test different readout options. We anticipate to make some progress in the design optimization of a 5x5 prototype based on the smaller 3x3 prototype for the NPS at JLab.

## **Future**

### **What is planned for the next funding cycle and beyond? How, if at all, is this planning different from the original plan?**

For this funding cycle we plan to complete our goals from the previous FY17 cycle and also try to make progress beyond that as budget constraints allow. ***Our highest priority is to determine ways to reduce the constant term, which includes nonlinearities in light collection that are in part properties of the crystal itself.*** In our January 2017 report we demonstrated that it needs to be on the order of 0.5% to make a clear positive impact on EIC physics. Our activities will thus include the *continuation of our crystal characterization studies* with emphasis on properties that affect the constant term (e.g. surface properties) and the *construction of a prototype* to evaluate limiting resolutions and to test different readout options. Specific activities are listed below.

- **Crystal characterization for crystal specification and impact on EIC detector performance, e.g. on the constant term**

- Characterize, including chemical analysis, 460 SICCAS crystals being produced in 2017 in collaboration with the NPS project. In anticipation of this next crystal testing phase and with support from the universities and laboratories, both CUA and IPN-Orsay have been actively procuring components and allocating space. This will allow us to perform chemical analysis and test the optical properties and the homogeneity of crystals produced at SICCAS and procured through synergy with the VSL and the NPS project at JLab. The results are an essential aspect required to quantify crystal-to-crystal variations and possibly understand their origin, and would thus provide a measure of the quality that can be achieved by that vendor. Feedback to vendors on influence of doping, impurities, defects on crystal quality is essential in this process.
  - Evaluate influence of crystal surface properties on constant term
  - Evaluate crystal-to-crystal variation of later growth cycle Crytur crystals, which are expected to have higher impurity concentrations
- **Construct a prototype to establish limiting energy and position resolution, and, together with simulations and crystal characterization, explore options to reduce the constant term.**
    - We plan to use the prototype together with simulations to evaluate contributions to the overall resolution and reducing the constant term including uniformity of crystal response and statistical fluctuations of containment losses. These studies will naturally include calibration of the precision among crystal stacks, dependence on incidence angle and spacing between the crystals.
    - Energy and position resolution can be established in test beam. The prototype could be calibrated with the tagged photon beam at Jefferson Lab. The basic principle of this test program is as follows. One tags the bremsstrahlung produced by a monoenergetic electron beam up to 11 GeV. After bremsstrahlung emission, the electrons are analysed by the magnetic spectrometer of the tagger requiring a coincidence of the bremsstrahlung photon with the corresponding electron in the focal plane. The NPS 3x3 PbWO<sub>4</sub> (or the envisioned EIC 5x5 prototype) array is composed of 9 (25) 200mm long rectangular crystals of 20x20 mm<sup>2</sup> cross section. It would be located at a position downstream of the radiator. A set of collimators can be used to control the beam spot on the front face of the crystals. The crystal matrix could be moved via remote control in two dimensions perpendicular to the axis of the collimated photon beam by stepping motors to perform a relative calibration of each detector element. This technique has previously

been used successfully for the Primex HyCal and at MAMI for tests of PANDA ECAL prototypes.

- **Investigate different readout systems and influence on the constant term**
  - We have started exploring PWO readout with SiPM and/or APDs. However, long-term stability and noise is a concern. Since the area to be instrumented is relatively small and not directly inside a magnetic field, PMTs, if can be shielded, may be a viable option as well. We plan to investigate these different readout options with the prototype.

Assuming that our FY18 crystal quality tests are completed successfully and one or two vendors capable of producing such crystals have been identified, the crystal calorimeter R&D will focus in subsequent years on the optimization of geometry, cooling and choices of readout system of the endcap inner crystal calorimeter. Cooling and choice of temperature are important aspects for crystal calorimetry. The choice of temperature balances light output and radiation recovery. Cooling techniques have been explored for the NPS project based on PANDA and CMS. The type of cooling and avoiding condensation depend to some extent on environmental factors. Our planned future R&D will explore how cooling could be achieved for the inner endcap calorimeter for EIC. Another reason for cooling is the reduction of noise in the readout system. Our initial studies with a SiPM-based readout have shown significant effects of noise at room temperature emphasizing the need for cooling. Our future R&D activities will also explore if cooling is the optimal choice to reduce readout noise and if it is how to implement such a system.

### **What are critical issues?**

At this stage, the most critical issues are to complete the FY17 activities and explore options to reduce the constant term. Crystal characterization will address fundamental questions about the crystal-to-crystal variation of crystals procured from SICCAS through synergy with the VSL and the NPS project, as well as the impact of systematic uncertainties between measurements. The construction of a prototype and availability of a sufficient number of quality crystals is critical. The prototype will allow for studies of the crystals in test beam and measure the actual energy and position resolution, to investigate possible reductions of the constant term, and to test different readout systems. The crystal and crystal prototype measurements would provide essential information on crystal specifications and their impact on EIC detector performance.

## **Budget Scenarios and Impact Statement:**

Our three main goals over the next year are: 1) continuing crystal characterization for crystal specification and impact on EIC detector performance, 2) construction of a prototype to establish limiting energy and position resolution, and, together with simulations and crystal characterization, explore options to reduce the constant term, and 3) investigation of different readout systems and influence on the constant term.

In the case of a 20% cut, we would have to delay the construction and testing of the prototype. We would be able to continue our crystal characterization studies but at lower efficiency. This limited continuation, even with a 20% cut, is enabled with the majority of our activities funded by the NPS project and internal funds. We would also be able to continue our general studies of different readout options.

In the case of a 40% cut, we would not be able to continue our crystal characterization studies. Our focus would mainly shift towards the NPS project, which would be the funding source for these activities, and we may only provide information relevant specifically for EIC. We would attempt to continue our general studies of different readout options at lower efficiency. These would proceed at significantly reduced efficiency regarding EIC. Construction and testing of the prototype is delayed.

The planned timeline and funds requested for R&D in FY18 (FY19) can be found in the tables below. As in the past we only request funding for materials and provide all labour for the proposed activities. The indirect cost rate at CUA is 58%. The fringe benefit rate is 23.75% on faculty/staff and 7.065% on student salaries. However, all labour in this project is supported by external sources other than EIC. We request \$38k for components and construction of a prototype needed to establish the limiting resolutions of the crystals and to explore ways to reduce the constant term in the resolution function. We also request \$21k for technical support needed in the construction and testing of the prototype and \$30k to procure 10 crystals from Crytur to instrument it. \$28k of travel support are requested to support trips to JLab to test the prototype. For testing alternative readout systems (APD, SiPM, PMT) with a prototype we request \$31k to purchase parts.

For the remaining part of the DAQ system, a complete portable DAQ system called RCDAQ can be provided at no cost by the sPHENIX Experiment. RCDAQ is a framework that is capable of reading out a large variety of hardware, including a number of commercial CAEN digitizer boards, the PSI DRS4 evaluation board, the CERN/RD51 SRS system, several Struck Flash ADCs, as well as custom hardware such as the digitizer boards designed for the sPHENIX calorimeters. RCDAQ has been the standard DAQ system for virtually all EIC-related lab setups at BNL, Stony Brook, Yale, and other institutions, and has been used for virtually all EIC-R&D test beam setups at Fermilab, such as the studies with GEM detectors and tests of various calorimeter modules read out with photomultipliers or SiPMs.

**Table 1.** 100% funding

Item	FY18 (\$K)	FY19 (\$)
Procure crystals from Crytur	30	10
Technical Support	21	18
Parts for prototype and construction	38	
Travel	28	28
Parts for cooling system		38
Parts for readout system	31	32
<b>Total</b>	<b>148</b>	<b>126</b>

**Table 2.** Scenario 20% cut

Item	FY18 (\$K)	FY19 (\$)
Procure crystals from Crytur	20	22
Technical Support	21	18
Parts for prototype and construction	25	11
Travel	26	28
Parts for cooling system		38
Parts for readout system	26	39
<b>Total</b>	<b>118</b>	<b>156</b>

**Table 3.** Scenario 40% cut

Item	FY18 (\$K)	FY19 (\$)
Procure crystals from Crytur	10	30
Technical Support	21	18
Parts for prototype and construction	25	13
Travel	16	40
Parts for cooling system		38
Parts for readout system	17	54
<b>Total</b>	<b>89</b>	<b>193</b>

**Table 4.** Funding by Institution (100% funding scenario).

Institution	FY18 (\$K)	FY19 (\$k)
CUA	58	52
JLAB		
BNL	32	22
Caltech		
IPN Orsay	58	52
Yerevan		
<b>Total</b>	<b>148</b>	<b>126</b>

For the reduced funding scenarios, its impact on crystal procurement, technical support, parts and construction of the prototype and travel would mainly be absorbed by CUA and Orsay, while the impact on the readout system would mainly be absorbed by BNL.

**Table 1** R&D Timeline and Deliverables

Deliverable	FY18 by Quarters				FY19 by Quarters			
	Q1	Q2	Q3	Q4	Q1	Q2	Q3	Q4
Procure crystals from Crytur	X	X						
Crystal quality tests	X	X	X	X				
Radiation Damage studies	X	X	X	X				
Construct prototype		X	X					
Test prototype				X	X			
Calorimeter configuration				X	X			
Cooling system studies						X	X	X
Readout system				X	X			
Readout noise reduction						X	X	X

**Manpower**

A list of existing manpower is shown below. All of the participants are supported by external funds and *not* through the EIC R&D program.

**IPN-Orsay**

M. Josselin  
F. Georges  
G. Hull  
C. Munoz-Camacho

**CUA**

D. Griggs, high school  
A. McShane, high school  
S. Roustom, high school  
S. Ali, graduate student  
R. Trotta, graduate student  
A. Vargas, graduate student  
M. Carmignotto, postdoc  
A. Mkrтчyan, postdoc  
T. Horn  
I. Pegg  
Vitreous State Laboratory

**Yerevan**

H. Mkrтчyan  
V. Tadevosyan

**BNL**

C. Woody  
S. Stoll  
M. Purschke

**Caltech**

R-Y Zhu

## Publications

C. Munoz-Camacho et al., “*R&D for high resolution calorimetry at the future Electron-Ion Collider*”, Presentation at the XVIIth International Conference on Calorimetry in Particle Physics, 15-20 May, 2016, Daegu, South Korea

Through synergy with the NPS project at JLab:

R. Trotta et al. “*Exclusive reactions and the PbWO<sub>4</sub>-based Inner Calorimeter for the Electron-Ion Collider*” presentation at the APS April 2017 meeting, Washington, DC

T. Horn, C. Munoz-Camacho, C. Keppel, I. Strakovsky et al., arXiv:1704:00816 (2017) “*Workshop on High-Intensity Photon Sources (HIPS2017) Mini-Proceedings*”

T. Horn et al., J.Phys. Conf. Ser. **587** (2015) 1, 012048 “*A PbWO<sub>4</sub>-based Neutral Particle Spectrometer in Hall C at 12 GeV JLab*”

T. Horn et al. “*Physics Opportunities with the Neutral Particle Spectrometer in Hall C*”, presentation at the APS DNP 2015 Fall meeting, Santa Fe, NM

## External Funding

- All of the FTEs required for working towards finalizing the crystal test setup and crystal characterization are provided by CUA/IPN-Orsay or external grants. The absence of any labour costs makes this proposed R&D effort extremely cost effective.
- The 2014 and 2015 SIC crystals, as well as 460 SIC crystals produced in 2017 are provided through synergistic activities with independent research for the Neutral Particle Spectrometer (NPS) project at JLab.
- The expertise and use of specialized instruments required for crystal characterization and their chemical analysis, as well as additional crystals samples are made possible through collaboration with the Vitreous State Laboratory (VSL) at CUA that is also collaborating on the NPS project. The VSL has trained and experienced staff and procedures already in place requiring no additional setup overhead beyond what is required for finalizing the crystal test setup, chemical analysis, prototype construction, and procuring crystals.

Efforts related to crystal studies as described here were accomplished with external funds through synergistic activities with the NPS project at JLab. Additional funds and facilities for crystal characterization were provided by the Vitreous State Laboratory at CUA. Salaries and wages were provided by private external grants from the individual principal investigators, e.g., IPN-Orsay, Yerevan, and the National Science Foundation.

## ***Synergies between HEP and NP detector R&D activities in the US***

Our studies suggest that PbWO<sub>4</sub> is the best option for the EIC crystal calorimeter providing the means for particle identification and resolution required by EIC science. At this time, we are not proposing to study any other crystals. However, we note the recent interest in the HEP community in BaF<sub>2</sub>, a scintillating crystal suitable for HEP science. Because of its fast scintillation light with sub-ns decay time, the HEP community is investigating a BaF<sub>2</sub> crystal based calorimeter to face the challenges of a very high event rate and a severe radiation dose expected in future HEP experiments. A calorimeter design has been developed for the Mu2e experiment based on BaF<sub>2</sub> crystals readout with solar-blind UV sensitive avalanche photo-diodes that efficiently collects the very fast UV component (~220 nm) of the scintillation light with sub-ns decay time while suppressing the slow component near 300 nm with 600 ns decay time. R&D has been also carried out to suppress the slow scintillation component by introducing rare earth doping in BaF<sub>2</sub> crystals. Recent progress in yttrium doped BaF<sub>2</sub> shows a significant increase in the Fast/Slow ratio from 1/5 to 5/1, while maintaining the amount of the fast light in BaF<sub>2</sub> unchanged. We plan to follow these developments closely and to explore the possible need for this type of performance for future high resolution crystal calorimeters.

## **APPENDIX:**

### ***PbWO<sub>4</sub> crystal characterization***

At CUA, both longitudinal and transverse transmittance was measured using PerkinElmer Lambda UV/Vis spectrophotometers with double beam, double monochromator, and a large sample compartment. The spectrometers allow for measurements of the transmittance and absorption between wavelengths of 250 to 2500 nm with 1 nm resolution. To measure the 20 cm long crystal samples the spectrometer compartments were modified with a horizontal positioning slide and a programmable stepper motor. The systematic uncertainty in reproducibility of the transmittance measurements is on the order of 0.2%. The light yield was measured with a Photonis XP2262 PMT with a bi-alkali lime glass window. For the light yield measurements, a collimated Na-22 source was used to excite the samples. The light yield was measured at a constant temperature of 18°C controlled to better than 1°C. Options for calibrating the PMT for inter-laboratory comparisons are being explored. The systematic uncertainty due to temperature control is better than a few %/°C. Radiation resistance measurements were carried out in collaboration with the Vitreous State Laboratory (VSL). These include radioactive sources and an X-ray irradiation system. Material characterization including determination of trace element impurities, defects, oxygen vacancies and structural analysis is also carried out in collaboration with the VSL. These studies use a combination of different instruments owned by the VSL, e.g., XRF, TEM and SEM, as well as Raman spectroscopy.

At IPN-Orsay a setup to measure optical transmittance (both longitudinal and transverse) and a setup to measure crystal light yield and timing were commissioned successfully. Light yield at different transverse positions along the crystals are measured using a <sup>137</sup>Cs collimated source. Fig. 1 shows a typical spectrum and measurement performed on a PANDA crystal. Through collaboration with the Laboratoire de Chimie Physique at Orsay the group has access to a panoramic irradiation facility based on 3000 Cu Co-60 sources. This facility can provide dose rates ranging from 6 to 5000 Gy/h. Thus, high total doses can be accumulated in a short period of time and the effect of different photon irradiation rates can also be studied. In addition, IPN-Orsay houses several beam facilities that can be used to further study the effects of radiation on PbWO<sub>4</sub> blocks. Firstly, a 50 MeV electron facility (ALTO) can provide up to 1 microA of electrons that can complement the irradiation tests made with photon sources. Secondly, a proton (and several ions) accelerator of the “Van de Graaf” type (Tandem) can provide proton energies in the range of tenths of MeV. This facility is also readily available and will provide information on the crystal damage induced by hadrons, important for the future EIC.

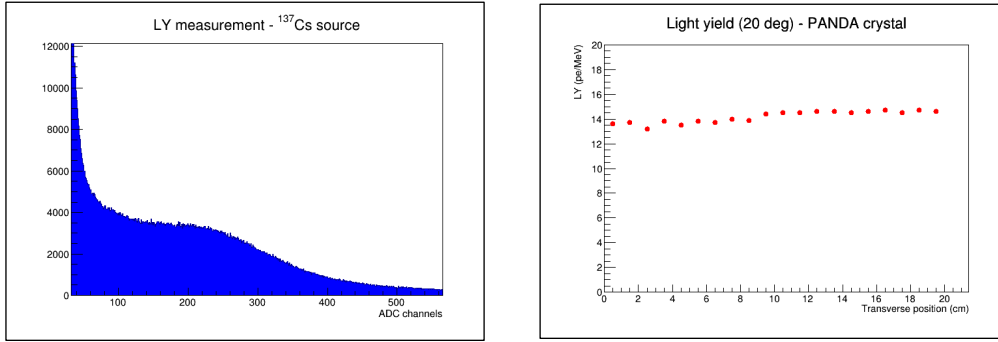


**Fig. 1:** Light yield measurements at IPN-Orsay on PANDA crystals using a  $^{137}\text{Cs}$  source.

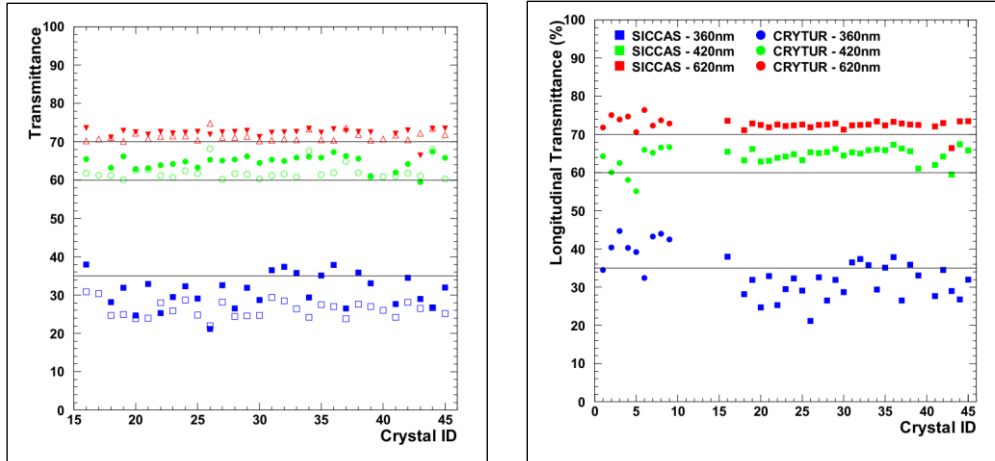
Table 4 summarizes the methods used to characterize crystals and availability of instrumentation. For guidance we also list the NPS requirements on the crystals, which is anticipated to be similar though perhaps stricter on radiation hardness than those for the EIC.

**Table 4:** Crystal specification parameters, NPS requirements, methods used in the characterization and availability of the instrumentation at different institutions.

Parameter	Unit	NPS Required	Inform. Source	Institutions
Light Yield (LY) at RT (90% within 100 ns gate at RT, for all sides polished crystals)	pe/MeV	$\geq 15$	Light yield measurement with Na-22 source or cosmics in temperature-controlled darkbox	CUA IPN-Orsay
LY uniformity between blocks	%	<b>10%</b>	Same as above	CUA IPN-Orsay
LY(100ns)/LY(1 $\mu$ s)	%	<b>&gt;95</b>	Same as above, but with different gate widths	CUA IPN-Orsay
Longitudinal Transmission at $\lambda=360$ nm at $\lambda=420$ nm at $\lambda=620$ nm	% % %	$\geq 35$ $\geq 60$ $\geq 70$	Perkin-Elmer Lambda 950 Perkin-Elmer Lambda 750 Varian Cary 5000 Ocean Optics Fiber spectrometer	CUA/VSL IPN-Orsay
Transverse Transmission and LY uniformity along crystal	%	<b>10</b>	Perkin-Elmer Lambda 950 Perkin-Elmer Lambda 750 Varian Cary 400 Ocean Optics Fiber spectrometer	CUA/VSL IPN-Orsay
Inhomogeneity of Transverse Transmission $\Delta\lambda$ at T=50%	nm	$\leq 5$		
Induced radiation absorption coefficient	$\text{m}^{-1}$	<b>&lt;1.0</b>	Faxitron CP 160 Co-60 source	CUA/VSL IPN-Orsay

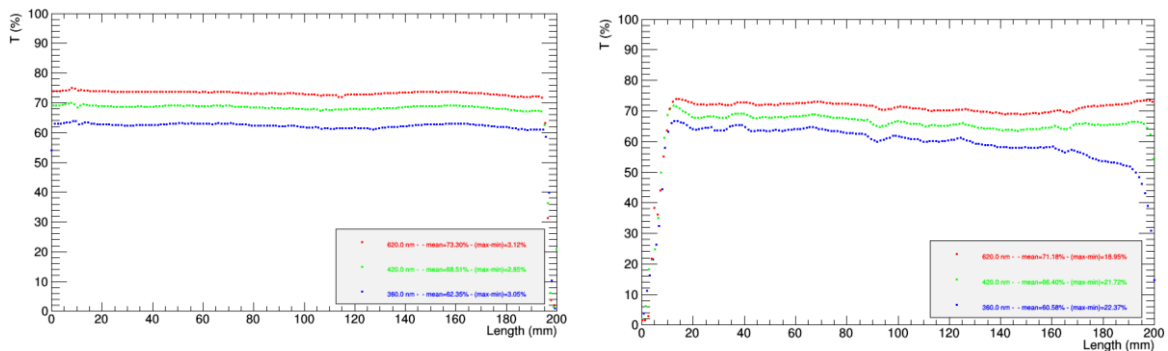
<b><math>\Delta k</math> at <math>\lambda=420</math> nm and RT, for integral dose &gt;100 Gy</b>			Electron beam Proton beam	Giessen U. IAC
<b>Mean value of dk</b>	<b>m<sup>-1</sup></b>	<b><math>\leq 0.75</math></b>		
<b>Tolerance in Length Tolerance in sides</b>	<b><math>\mu\text{m}</math> <math>\mu\text{m}</math></b>	<b><math>\leq \pm 150</math> - <math>\leq \pm 50</math></b>	Laser based measurement	JLab CUA
<b>Surface polished, roughness Ra</b>	<b><math>\mu\text{m}</math></b>	<b><math>\leq 0.02</math></b>	XRD, Raman microscope, AFM	CUA/VSL
<b>Tolerance in Rectangularity (90°)</b>	<b>degree</b>	<b><math>\leq 0.1</math></b>		JLab CUA
<b>Purity specific. (raw material)</b>			ICP-MS, ICP-ES, DCP-ES, MS, GC, IC, XRF, FT-IR, LA- ICP-MS	CUA/VSL company
<b>Mo contamination</b>	<b>ppm</b>	<b>&lt;1</b>	ICP-MS, ICP-ES, DCP-ES, MS, GC, IC, XRF, FT-IR, LA- ICP-MS	CUA/VSL
<b>La, Y, Nb, Lu contamination</b>	<b>ppm</b>	<b><math>\leq 40</math></b>	ICP-MS, ICP-ES, DCP-ES, MS, GC, IC, XRF, FT-IR, LA- ICP-MS	CUA/VSL

Figure 2(left) shows a comparison of longitudinal transmittance measurements at CUA and results reported by SICCAS for a set of crystals produced in 2015. At wavelength 620 nm the data are in good agreement and crystal transmittance meets our requirements. At wavelength 360 and 420 nm the measurements at CUA seem to be systematically higher than those from SICCAS. Requiring a longitudinal transmittance of greater than 60% at 420 nm as for the JLab NPS project the crystal transmittance meets the requirements, while only 18% pass the specifications at 360 nm. Figure 2(right) shows the longitudinal transmittance of rectangular 20-cm long crystals produced at Crytur in 2016 in comparison to those produced at SICCAS in 2015 shown in Figure 2(left). Both sets of crystals perform well at 620 nm. At 360 and 420 nm about 20% of the Crytur crystals are below specification. The situation is reversed for the SICCAS set at 360 nm, where only 18% of the crystals pass. The results are consistent with cross checks of a subset of crystals carried out at Caltech. A different subset of the same crystal batch that was characterized at CUA and IPNO was tested at Giessen University through collaboration on the NPS project. The results showed that none of the crystals would pass the required limit at 420 nm. This is consistent with recent observation at PANDA, where only 12% of a recent 2015 produced subset of crystals passed the longitudinal transmittance criterion. The data acquired with different setups suggest a systematic offset between the CUA and Caltech (2.4% higher) and Giessen University (20% lower) measurements. These offsets need to be understood for interpreting crystal quality and for generating vendor specifications. Ongoing measurements at IPN-Orsay are expected to shed light on this.



**Fig. 2:** Longitudinal Transmittance of SICCAS crystals produced in 2015 and Crytur crystals produced in 2016. (left) a comparison of measurements at CUA (solid) and results reported by SICCAS (open); (right) transmittance measured at CUA and Giessen U. for Crytur crystals (solid circles) and transmittance measured at CUA for SICCAS crystals (solid squares).

A crystal-to-crystal variation in transverse transmittance up to 10% for wavelengths 360 nm, 420 nm, and 620 nm is considered within specifications. Variations in transverse transmittance of more than 15% results in rejection of the crystal sample. Examples of the homogeneity of the transverse transmittance along the crystal length are shown in Fig. 3. For the subset tested thus far, the variation in transverse transmittance is tolerable for most crystals.



**Fig. 3:** Variation of the transverse transmittance along the crystal for a sample that passes specification (left) and a sample that was rejected (right).

For the NPS project the acceptable limit on the light yield at 18 °C is 15 pe/MeV. If one applies this criterion to a subset of SICCAS crystals produced in 2014 and 2015, about 45% of the samples will pass the specification limit. This fraction is consistent with a cross check of a subset of the same crystals carried out at Giessen University and another subset of the same crystals carried out at Caltech. In both cases, about 50% of the tested subsets passed specification. The light yield measurements carried out on the same subset of crystals at CUA and Caltech and Giessen agree to within 1 pe/MeV. We also tested the light yield of 28 full-sized

Crytur crystals of different geometries produced in 2016. A representative spectrum is shown in Fig. 4 (right). Only 20% of the crystals with ID up to 12 pass the light yield requirement. The non-uniformity of the light yield along the crystal appears to be tolerable. The low value of the light yield could be due to high doping levels. Lower doping levels were investigated and improved the light yield of the crystals as seen for crystals IDs 13-16. Crystals with higher IDs are of a different geometry (T11), which increases light yield through focusing. While beneficial for higher light yields, this geometry also introduces aspects of non-uniformity, which would impact the constant term in the resolution function. Our ongoing studies focus on determining the crystal-to-crystal variation in the light yield and possibly understanding the origin of it, e.g. doping levels, as well as the impact of geometry on resolution requirements.

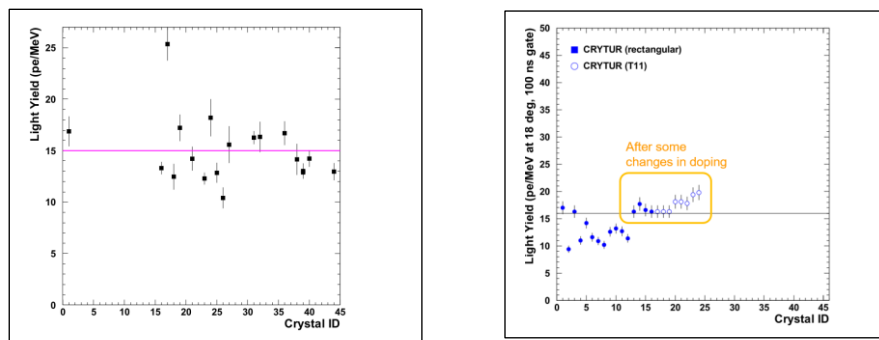


**Fig. 4:** Light yield for a subset of crystals produced at SICCAS (left) and Crytur (right) in 2014/15. The variation between crystals is large for SICCAS. The overall light yield is low for Crytur, which could be due to high doping concentrations. The variation of the light yield along the crystal is tolerable.

Fig. 5 shows the results of crystal performance tests in a radiation environment quantified by the absorption coefficient for a subset of 2015 produced SIC crystals. An absorption coefficient of better than  $1.1 \text{ m}^{-1}$  at 420 nm is required to pass NPS specifications. The PANDA requirements are even stricter. At 420 nm about 50% of this subset of crystals pass the NPS radiation hardness requirement. Two different subsets of 2014 produced SIC crystals were tested for radiation hardness at Caltech and Giessen U. The subset tested at Caltech was determined to be radiation hard, 80% of the subset tested at Giessen U. passed the radiation resistance requirement. Both of these subsets were also tested at CUA. The results were consistent. We also tested 28 crystals Crytur crystals produced in 2016. Out of this set 79% passed NPS and PANDA specifications. Ongoing studies focus on batch-to-batch crystal variations of both SICCAS and Crytur crystals, which has been a major concern in the past and could impact resolution through introduction of non-uniformities in the response.

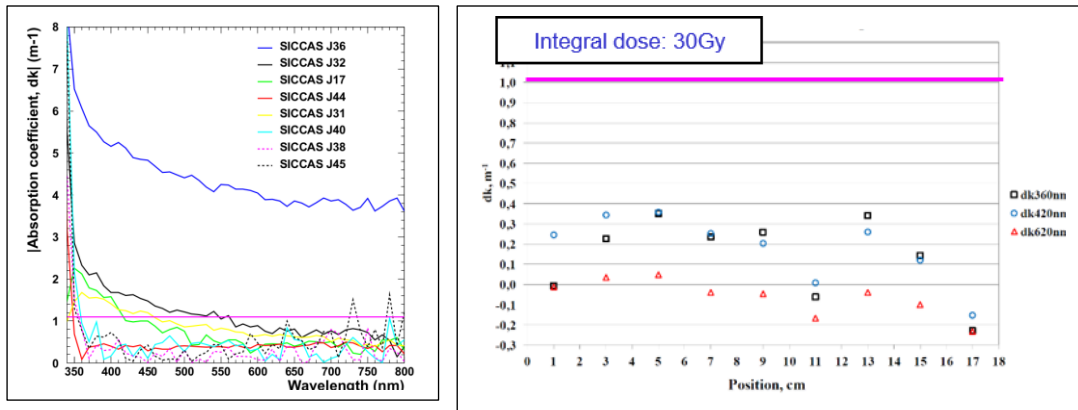


**Fig. 5:** The absorption coefficient,  $dk$ , of a subset of SICCAS crystals produced in 2015 and a subset of Crytur crystals produced in 2016. Assuming the NPS specification of  $dk$  to be better than  $1.1 \text{ m}^{-1}$  at 420 nm, about 50% of the SICCAS subset pass the requirement, 79% of the 28 tested crystals pass the radiation resistance requirement.

### Material characterization

To understand variations in  $\text{PbWO}_4$  characteristics like transmittance, light yield, decay times and radiation hardness material characterizations are being carried out at CUA. As an example, our earlier X-Ray Fluorescence (XRF) results of a SICCAS crystal sample with lower optical transmittance than expected showed that the sample consists of two phases and the observed low optical transmittance was due to surface oxidation. This is important information to communicate to the vendors. Furthermore, non-optimal Pb/W ratios have been shown to be related to poor radiation hardness. The trace element Mo is an impurity in  $\text{PbWO}_4$  crystals and can generally be related to slow components. To establish another method, a SICCAS sample produced in 2014 was analysed with Inductively Coupled Plasma Mass Spectroscopy (ICP-MS). The result showed impurities on the few percent level. However, no data on transmittance, light yield, or radiation resistance are available for this sample. Additional tests with samples of poor performance are underway.

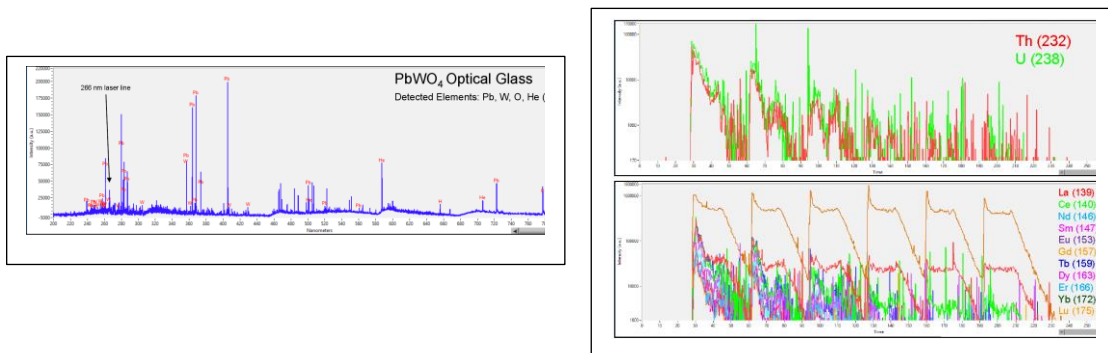


**Fig. 6:** Preliminary results of a non-destructive trace element analysis with LA-LIBS (left) and LA-ICP-MS (right)

Typical crystal samples have dimensions that are not compatible with chemical analysis sampling requirements resulting in damage to the crystal during

sampling. We have thus explored several non-destructive sampling methods including portable x-ray systems for large samples, e.g. coupled with a silicon drift detector (SDD) as used in archaeology, the arts (to quantify bulk and trace elements in ink), and medicine, scanning electron microscopy coupled with energy dispersive x-ray spectroscopy (SEM-EDS), as well as laser ablation (LA) in conjunction with ICP-MS, laser induced breakdown spectroscopy (LIBS) and ICP-AES (inductively coupled plasma atomic emission spectroscopy). The latter is a method in which the sample is created with a laser beam. We used a J200-EC tandem system with 150  $\mu\text{m}$  spot size and a 10 Hz laser. The ablated particles are analysed with methods like LIBS or ICP-MS, where the mass spectrometer performs both elemental and isotopic analysis.

Fig. 6 shows initial results of a SICCAS sample. Left is a typical LIBS spectrum. When the plasma cools, the excited electronic states return to their ground states emitting light with discrete spectral peaks in the process. The light is coupled with an intensified CCD camera and spectrometer for time-resolved spectral analysis. Each element in the periodic table is associated with a unique peak in the spectrum. By identifying the different peaks, the sample's chemical composition can be determined. Characterization of selected full-size  $\text{PbWO}_4$  samples produced by SICCAS in 2014 and 2015 and Crytur in 2016, as well as late production cycle crystals, is ongoing. We are also investigating crystal surface properties in relation to ways to reduce the constant term.

### ***Impact of impurities - CRYTUR late growth cycle production***

Due to the details of the crystal growth process later production crystals are expected to contain a higher level of impurities, which affect crystal performance. To determine if later production crystals would be suitable for EIC, we obtained one Crytur crystal from the 5<sup>th</sup> production cycle. Initial results are shown in Fig. 7. The crystals' transmittance is comparable to that of earlier tested Crytur crystals and the sample seems to be radiation hard. However, the light yield is with  $\sim 10$  pe/MeV would not pass the NPS (or PANDA) requirements. Additional tests including a chemical analysis of the impurity level are ongoing and results will be communicated to the vendor.

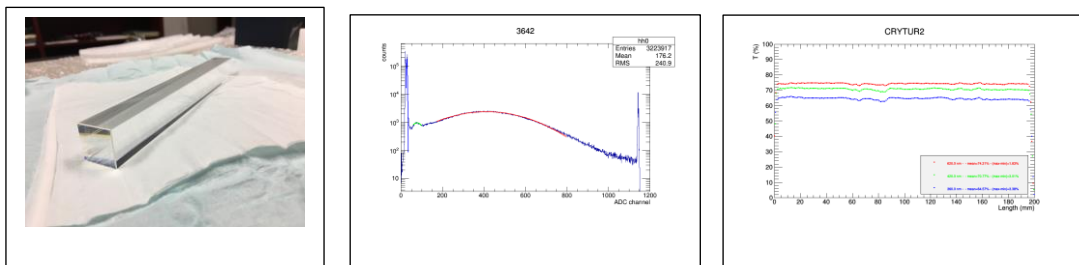


**Fig. 7:** Characterization of one Crytur 5<sup>th</sup> cycle production crystal. The initial result for the light yield at 18 degrees is 10 pe/MeV and would not pass the NPS requirement. The transverse transmittance shown on the right is comparable to earlier measured Crytur crystals and passes specification.

### ***Measurement of light output of PWO crystals with photodiodes***

In our earlier studies we showed that measurement of the light yield of PWO with SiPMs is feasible and at a level sufficient to provide better than  $2\%/\sqrt{E}$  in terms of energy resolution. More recently we presented the results of a beam test.

We also started exploring readout with APDs. A single crystal prototype with is shown in Fig. 8(left). Initial studies show that the APD-based readout is extremely sensitive to background noise and to temperature. Our initial results of the temperature dependence are shown in Fig. 8(right). The relative error of the data provides a representation of the APD signal fluctuation due to temperature.

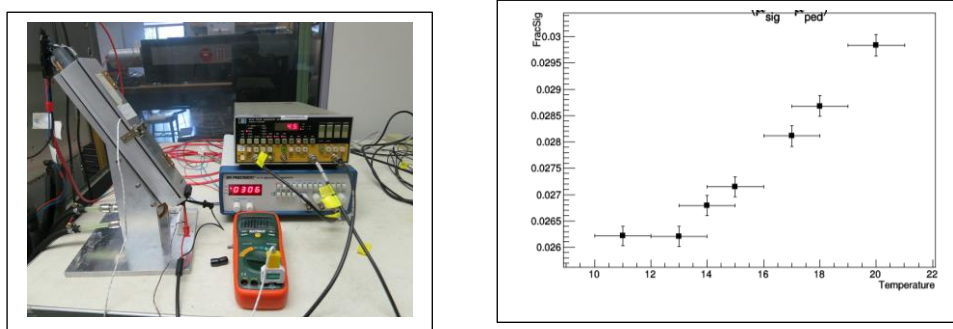


**Fig. 7:** Test of an APD-based readout system with a single crystal prototype.

### ***Students and young scientists***

Over the last year, 3 high school, 1 undergraduate, and 4 graduate students have participated in different aspects of the project. Students constructed and commissioned instrumentation used for crystal characterization. Last year, three of the high school and undergraduate students had the opportunity to present their results at the APS DNP 2016 meeting.

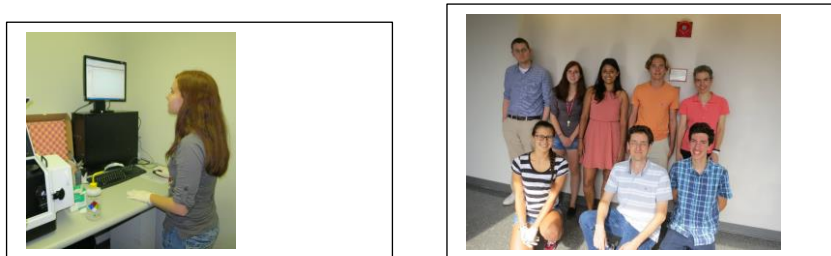


**Fig. 8:** Students at CUA.